

OPTICAL AND ELECTRICAL PROPERTIES OF NON- AND X-RAY
IRRADIATED PMABB

M. GAAFAR and S. M. KHALIL

Department of Physics, Faculty of Science, Alexandria University, Egypt

Received 6 July 1998 ; revised manuscript received 7 December 1998

Accepted 6 July 1999

Studies of the optical and electrical (ferroelectric, electrical conductivity) properties of non- and X-ray-irradiated pentakis undecabromodibismuthate (PMABB) orthorhombic crystals were made. The crystal is anisotropic, weakly positively birefringent and optically biaxial with the optical angle $2V = 72^\circ 15'$. The temperature dependence of linear birefringence $\Delta(\Delta n_c)$ in the temperature range from 295 K to 320 K shows an anomaly at the phase-transition temperature $T_c = 312$ K, in agreement with the published result. The spontaneous polarization P_s seems slightly large in comparison with those of other ferroelectrics, owing to the strengthened packing along the polar axis. The results show that the microscopic mechanism driving the phase transition has the same influence on the spontaneous birefringence $\delta_s(\Delta n_c)$ and on P_s in the compound. Effects of irradiation on the refractive indices and their dispersions as well as on the optical anisotropy and optical birefringence are studied. The coercive field E_c and the bias field E_b build up during the irradiation, while P_s shows no change with the enhanced doses until the threshold irradiation ($D_0 = 4 \times 10^4$ rad) is reached, then it begins to decay in a fairly rapid manner. The results are discussed in terms of the conventional double-minimum potential energy used for the description of the ferroelectric mechanism. Measurements of the electrical conductivity σ in the same temperature range show an anomaly at T_c due to the generation of protonic carriers as a result of rotational motion of cations. The maximum σ -value at the threshold irradiation D_0 is observed and the variation of σ in the vicinity of D_0 was studied.

PACS numbers: 78.20.Fm, 63.75.+t, 77.80.Bh

UDC 537.874.32, 536.425

Keywords: pentakis undecabromodibismuthate, spontaneous polarization, refractive indices, optical birefringence, electrical conductivity

1. Introduction

Pentakis undecabromodibismuthate (PMABB) is one of new members of alkylammonium halogeno-bismuthate salts which show a number of interesting phase transitions arising from the possibility of rotational motion of cations [1–4]. It exhibits para-ferroelectric phase transition at $T_c = 312$ K. The structure is orthorhombic below and above T_c with space groups $Pca2_1$ and $Pcab$, respectively [3,5]. The packing is strengthened by the N-H-Br bonds between anions and cations along the c -axis, and consequently is responsible for the strong polar character in the ferroelectric phase in the direction of the c -axis [6].

The use of ferroelectrics as detectors and memories has created the need to study the effect of irradiation on physical properties of these materials [7–10]. Further measurements on the defected ferroelectric materials are very important for some practical applications. Defects generated in any crystalline lattice due to the irradiation cause deformation of the surrounding lattice and modification of the local fields. The extent of the crystal deformation depends on the nature of the defect, its site in the crystal and the host-defect interaction.

In our study of the physical properties of some interesting materials for industrial purposes [11–13], we investigated the optical and electrical properties of non- and X-ray-irradiated PMABB at temperatures around the phase-transition.

2. Experimental

Pentakis (methylammonium) undecabromodibismuthate (PMABB), of the chemical formula $[\text{NH}_3(\text{CH}_3)_5\text{Bi}_2\text{Br}_{11}]$ was prepared by the reaction of $(\text{BiO})_2\text{CO}_3$ with CH_3NHBr in concentrated HBr . The crystal was purified by repeated crystallization. Single crystals were grown from dilute HBr , and their composition was determined by elemental analysis. Initial elements of high purity (99.99%) were used to prepare the crystals.

Axial refractive indices n_a , n_b and n_c were measured at 298 K using the previously published methods [13]. The Becke test [14] was demonstrated at the extinction directions (axial directions of the orthorhombic configuration). Ferroelectric hysteresis loops were measured using the modified Sawyer-Tower circuit at a frequency of 50 Hz [15]. In some cases, reverse nucleation may have occurred before the reversal of the applied field. It could be observed either in the presence of internal or external stress, or, if the free charges below the crystal surface could not reach their new equilibrium distribution, during each half-cycle of the hysteresis loop. The effects could be minimized by cycling the loop at a very low frequency. The electrical conductivity σ was measured using the method described in our previous work [16]. The samples were irradiated at room temperature at the distance of 3 cm from the X-ray source. The X-ray tube was operated at 30 kV and with a current of 15 mA.

3. Results and discussion

The results for the refractive indices of PMABB at room temperature and the wavelength $\lambda = 250$ nm are $n_a = 1.712 \pm 0.031$, $n_b = 1.736 \pm 0.025$ and $n_c = 1.761 \pm 0.004$. The results show that the crystal is anisotropic, and the direction of the maximum index n_c is that of slow vibration that lies parallel to the strong NH-Br hydrogen bond. This direction is characterized by high refraction and high polarization. The direction of fast vibration (the minimum index n_a) is characterized by weak binding and low polarization. Orientation of the optical indi-

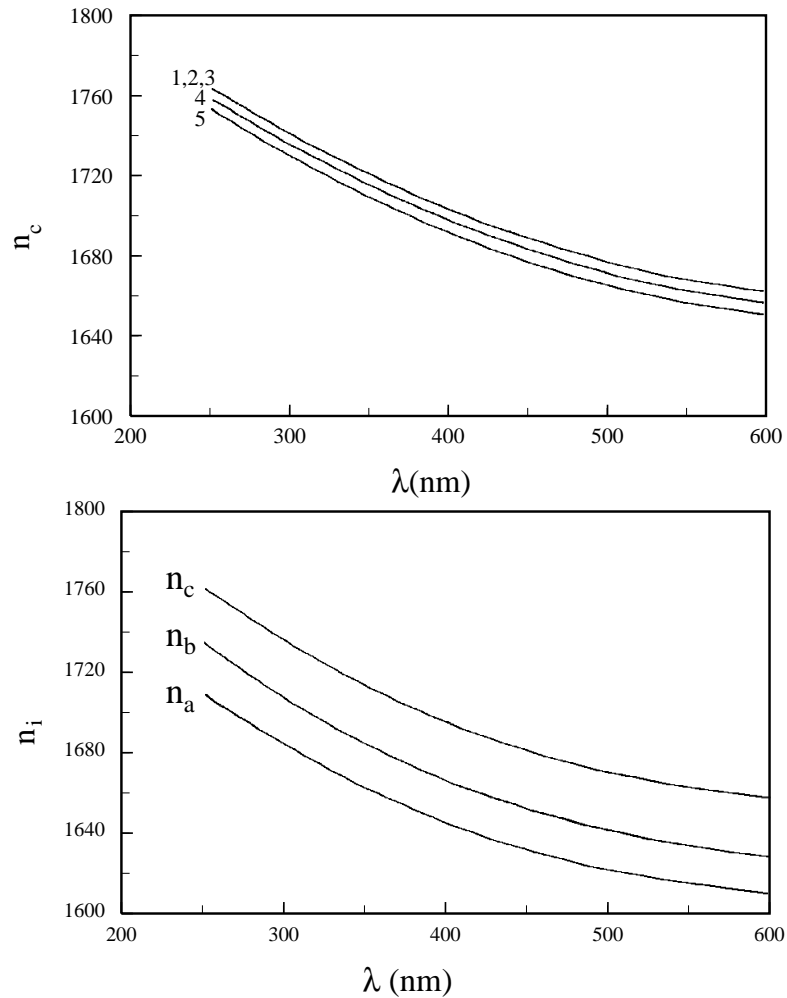


Fig. 1. Dispersion curves of the refractive indices at 298 K a) of the non-irradiated sample b) Variation of n_c for the non-irradiated sample (curve 1) and for irradiated samples: curves 2 and 3 for $D < D_0$ and curves 4 and 5 for $D > D_0$.

catix suggests weak positive birefringence with molecules of needle-like shape [17]. The result for the optical angle is $2V = 72^\circ 15'$, and the (010) plane is the optical axial one. The high refractive indices in the (010) plane show high polarization and indicate that it lies nearer to the molecular plane than to the axial plane. The high polarization in the molecular plane is attributed to the presence of the polarized Br ions and $(\text{CH}_3 - \text{NH}_3)$ groups, in which CH and NH ions are considered as one group causing the polarizabilities at the centre of the bond. This high polarization is confirmed by the strengthened packing through N–H–Br hydrogen bonds between anions and cations along the polar axis of the compound [6].

Figure 1a shows the dispersion curves of the refractive indices n_a , n_b and n_c for non-irradiated samples at room temperature. Figure 1b shows the effects of irradiation on n_c for a sample: curve 1 shows the values prior to irradiation and curves 2 – 5 after irradiation. Curves 2 and 3 show no change in n_c for low doses ($D \leq D_0 = 4 \times 10^4$ rad) within the limits of accuracy of the measurement (1×10^{-3}), which is attributed to the competition of radiation annealing and radiation defects. Marked decrease of n_c for doses 6×10^4 rad and 9×10^4 (curves 4 and 5, respectively) is observed, when the internal displacement fields induced by radiation defects cause the changes via the electro-optical effects. Similar behaviour of n_a and n_b due to irradiation was observed. Irradiation changes n_i , $i = a, b, c$ in such a way that the crystals remain anisotropic, nearly like the non-irradiated ones, and the refractive indices continue to obey the relation $n_c > n_b > n_a$. This also holds for the results of measurement of dispersion, $\partial n_c / \partial \lambda > \partial n_b / \partial \lambda > \partial n_a / \partial \lambda$. The slight variations of the results for n_i depends on the orientation of the vector of the electric field, \vec{E} , of the light wave (the plane of polarization) with respect to the crystallographic axes. The temperature dependence of the linear birefringence $\Delta(\Delta n_c)$, in the temper-

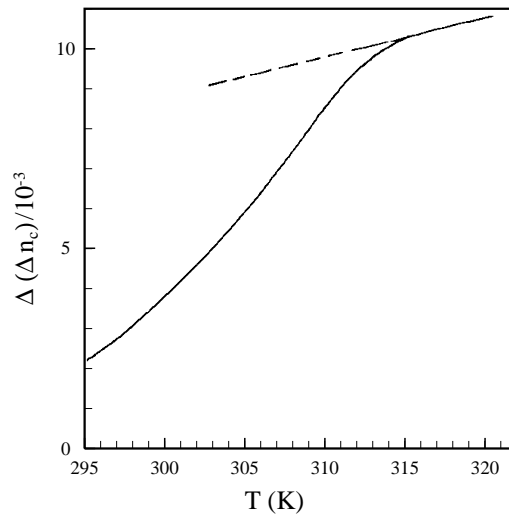


Fig. 2. Temperature dependence of linear birefringence $\Delta(\Delta n_c)$.

ature range from 295 to 320 K, determined by the HAUP method [19], shows an anomaly at the temperature T_c (see Fig. 2). The spontaneous birefringence $\delta(\Delta n_c)$, induced by the phase transition (see Fig. 3), was deduced by calculating the differences between the straight-line extrapolation of the high-temperature phase and of

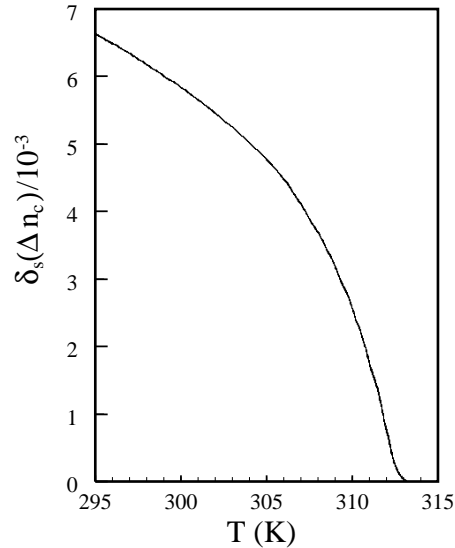


Fig. 3. Temperature dependence of spontaneous birefringence $\delta_s(\Delta n_c)$.

the measured results, as shown in Fig. 2. $\delta(\Delta n_c)$ shows a distinct smearing at T_c , which can be attributed to the crystal imperfections causing undefined blurring of the transition by the induced internal biasing fields. The temperature dependence of $\delta(\Delta n_c)$ is typical of a second-order transition [20].

Figure 4 shows the temperature dependence of the spontaneous polarization P_s which is equal to the saturation value of the electric displacement at zero field in the hysteresis loop. The values of P_s decrease gradually and reduce to zero at T_c . The high value of P_s of the ferroelectric PMABB, in comparison with those of other ferroelectrics, is attributed to the strengthened packing along the polar axis by the N–H–Br hydrogen bond between the anions and cations [6]. From Figs. 3 and 4, it appears that $\delta(\Delta n_c)$ scales nearly as P_s^2 . Hence, two hypotheses can be suggested. First, if $\delta(\Delta n_c)$ develops wholly due to the appearance of P_s , then the temperature of both of them (i.e., the temperature dependence of the effective quadratic electro-optic coefficient) is the same in the low-temperature phase. Second, the microscopic mechanisms causing the phase transition have the same influence on $\delta(\Delta n_c)$ and on P_s . The effect of irradiation shows no noticeable change in P_s , within the limits of the experimental errors, until the threshold irradiation dose D_0 is reached. For higher irradiation doses, P_s decreases rapidly. This means that at $D < D_0$, the whole crystal suffers a relatively minor amount of local damage, so that the hysteresis loop retains its entity throughout the initial stages of irradiation.

The increase of damages at $D > D_0$, which affects many neighbouring cells, tends to destroy the dipole coupling across these damaged regions, and hence reduces P_s .

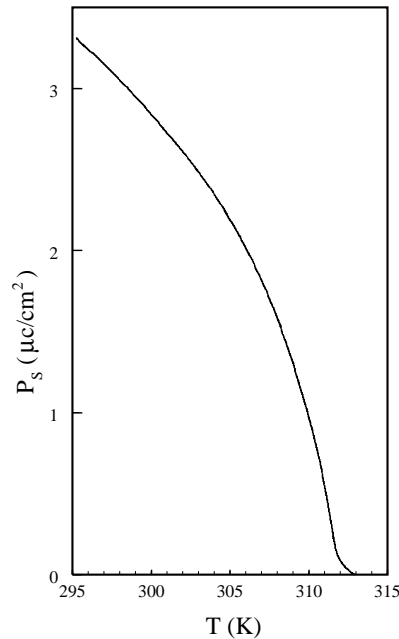


Fig. 4. Dependence of spontaneous polarization P_s on temperature.

These processes could possibly explain the variation of P_s with irradiation, but they would not account for the biasing effect. On the other hand, irradiation damage effects might be ascribed to a migration of the imperfections produced by irradiation into the domain walls [21]. Imperfections segregating in this way could trap the domain wall. Such a mechanism appears attractive in that one could readily account for the memory effects.

The ferroelectric mechanism of PMABB and the behaviour of P_s for different irradiation doses can be explained in terms of the phenomenological model [22,23], based on the potential energy diagram in which the ion responsible for the ferroelectric properties is in one of two minima in the undamaged state. The irradiation is supposed to modify one side of the potential energy with respect to the other. If, during the irradiation, the unoccupied minimum is steadily raised with respect to the other minimum, and the distance of the two minima remains unchanged, one can account for the initial constancy of P_s . If the unoccupied minimum is gradually obliterated, the crystal will become polar and non-ferroelectric, as confirmed by the persistence of the pyroelectric effect after the hysteresis loop deteriorates [24,25]. This explanation of the behaviour of P_s for different irradiation doses is not verified, and it is possible that another model will account more realistically for the observed effects.

Figure 5 shows the temperature dependence of the coercive field E_c , which is defined as the half-width of the hysteresis loop, whatever the value of the bias field. It decreases with increasing temperature and disappears at T_c . As a result of irradiation, E_c increases steadily until D_0 is reached, and declines for higher doses (see Fig. 6). Figure 6 illustrates also the increase of the bias field E_b (derived from

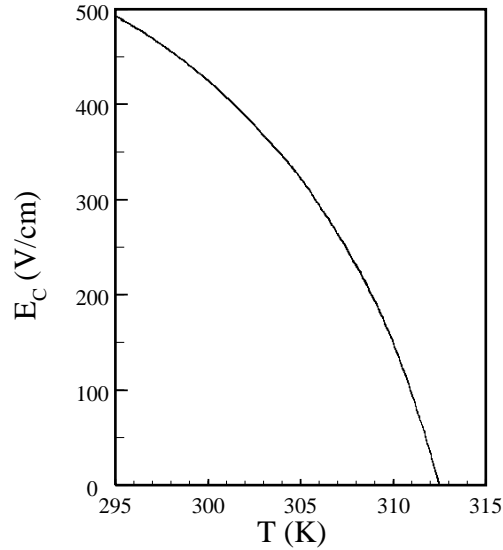


Fig. 5. Dependence of coercive field E_c on temperature.

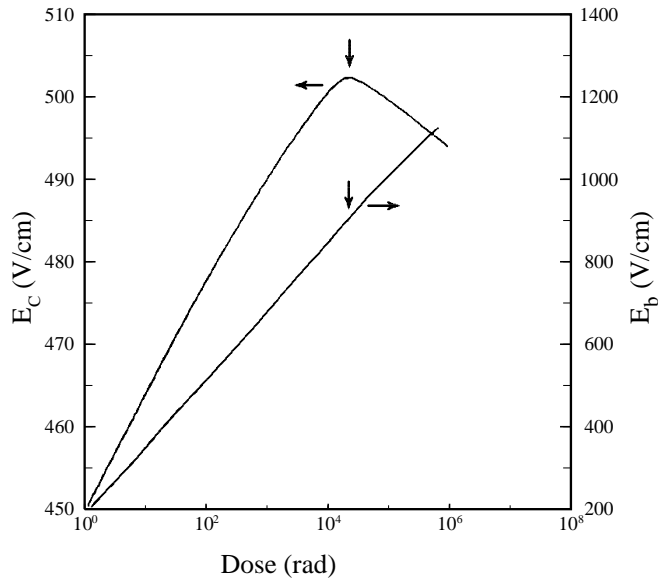


Fig. 6. Variation of E_c and E_b with irradiation dose at 298 K.

the measurements of the hysteresis loop) as a function of the irradiation dose. E_b shows a pronounced irradiation effect along the polar c -axis, and it refers in each case to the average of magnitudes of the bias fields of the subsidiary loops. E_b increases approximately linearly with the irradiation dose, though it is difficult to determine the behaviour after a long irradiation as the quality of the loops deteriorates.

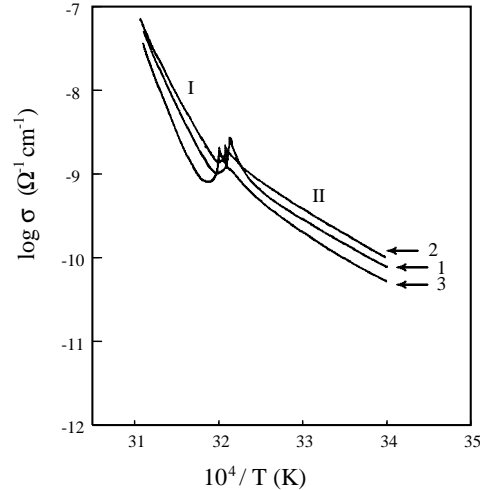


Fig. 7. Variation of $\log \sigma$ versus $10^4/T$ of the non-irradiated sample (curve 1) and of the irradiated samples (curve 2 for $D < D_0$ and curve 3 for $D > D_0$).

Figure 7 shows the dependence of electrical conductivity along the ferroelectric axis, σ , on temperature in the range from 295 to 320 K. The striking feature of the present result is a gradual transition at T_c , which is typical of the second-order transitions. The anomaly in σ at T_c is considered to be due to the rotational motion of methylammonium cations [6], which may generate an enormous amount of protonic carriers [26]. The dependence of σ on temperature shows two distinct regions (indicated in Fig. 7 by II and I, at temperatures below and above 312 K, respectively) which are characteristic of ionic crystals [27]. Except for the vicinity of the transition points, the rates of change of σ are very large both in region I and region II. The region I can be considered as the intrinsic region since the shown curves tend to merge at increasing temperatures. For lower doses, $D < D_0$, the effect of irradiation by damaging the chemical bonds and creation of some charged carriers with high mobilities, leads to an increase of σ . That is followed by the decrease of σ for higher doses ($D > D_0$), which is considered to be due to the dominant activity of the trapping centres.

4. Conclusion

The crystal PMABB is anisotropic, weakly positively birefringent and optically biaxial with the optical angle $2V = 72^\circ 15'$. Spontaneous polarization, P_s , is slightly

large due to the strengthened packing by the hydrogen bond along the polar c-axis. The microscopic mechanism driving the phase transition has the same influence on P_s and the spontaneous birefringence, $\delta_s(\Delta n_c)$. For irradiation doses $D < D_0$, P_s shows little change, but for $D > D_0$, P_s falls off in a fairly rapid manner. The results are discussed in terms of the double-minimum potential energy that is used for the description the ferroelectric mechanisms. The coercive field E_c and the bias field E_b increase with irradiation due to the changes of the internal fields. The electrical conductivity σ shows an anomaly at the transition temperature T_c due to the generation of the protonic charge carriers that is a result of the rotational motions of the cations in the crystals. For $D < D_0$, σ increases due to the creation of carriers with a high mobility, but for higher irradiation doses, $D > D_0$, it decreases due to the activities of the trapping centres.

References

- 1) R. Jakubas, L. Sobczyk and J. Lefevre, *Ferroelectrics* **100** (1989) 143;
- 2) R. Jakubas, *solid state comm.* **69** no. 3 (1989) 267;
- 3) R. Jakubas and L.Sobczyk, *Phase transitions* **20** (1990) 163;
- 4) J. Mróz and R. Jakubas, *Ferroelectrics* **118** (1991) 29;
- 5) J. Matuszewski, R. Jakubas, L. Sobczyk and T. Glowiak, *Acta Cryst. C* **46** (1990) 1385;
- 6) J. Lefebvre, P. Carpentier and R. Jakubas, *Acta Cryst. B* **47** (1991) 288;
- 7) P. Lock, *J. Appl. Phys. Lett.* **19** (1971) 390;
- 8) K. L. Bye and E. T. Keve, *Ferroelectrics* **4** (1972) 87;
- 9) K. L. Bye, P. W. Whipps and E. T. Keve, *Ferroelectrics* **4** (1972) 253;
- 10) C. Alemany, J. Mendiola, B. Jimenez and E. Maurer, *Ferroelectrics* **5** (1973) 11;
- 11) M. Gaafar, *Fizika A (Zagreb)* **5** (1996) 41;
- 12) M. Gaafar, T. G. Abdel-Malik, M. El-Shabasy and I. Mahmoud, *Indian J. Phys. A* **65** no. 4 (1991) 318;
- 13) M. Gaafar, M. A. Lasheen, A. A. Aly and A. M. Ahmed, *phys. stat. solidi (a)* **K 259** (1989) 111;
- 14) N. H. Nartshorne and A. Stuart, *Crystals and the Polarizing Microscope*, 2nd ed. (1950) p.225;
- 15) J. K. Sinka, *J. Sci. Instrum.* **42** (1965) 696;
- 16) T. G. Abdel-Malik, M. El-Shabasy, R. M. Abdel-Latif, M. E. Kassem and M. Gaafar, *Indian J. Phys. A* **65** no. 2 (1991) 1381;
- 17) E. Manghi, C. A. De Caroni, M. R. De Benyacar and M. J. De Alebedo, *Acta Cryst.* **23** (1967) 205;
- 18) V. Devarajan and A. M. Glazer, *Acta Cryst. A* **42** (1986) 560;
- 19) J. Kobayashi and Y. Uesu, *J. Appl. Cryst.* **16** (1983) 204;
- 20) S. Ushio, *J. Phys. Soc. Japan* **53** no. 9 (1984) 3242;
- 21) T. Mitsui and J. Furuichi, *Phys. Rev.* **90** (1953) 193;

- 22) Y. Onodera, Progr. Theor. Phys. (Kyoto) **44** (1970) 1477;
- 23) R. Blinc, J. Phys. Chem. Solids **13** (1960) 204;
- 24) A. G. Chynoweth, J. Appl. Phys. **27** (1956) 78;
- 25) A. A. Ballmann and H. Brown, Ferroelectrics **4** (1972) 189;
- 26) A. B. Lidiard, Handbuch der Physik **20** (1957) p. 246;
- 27) Y. V. Murty and P. S. Parasd, Solid State Comm. **15** (1974) 1619.

OPTIČKA I ELEKTRIČNA SVOJSTVA NEOZRAČENOG I RENDGENSKIM ZRAČENJEM OZRAČENOG PMABB

Proučavala su se optička i električna svojstva ortorombnih kristala pentakis undecabromodibismuthata (PMABB) prije ozračivanja i ozračenih s nekoliko doza rendgenskog zračenja. Kristali PMABB su anizotropni, malo pozitivno dvolomni i optički dvoosni s optičkim kutom $2V = 72^\circ 15'$. Spontana polarizacija P_s je relativno velika zbog snažnijeg slaganja vodikovim vezanjem duž polarne c-osi. Mikroskopski mehanizmi koji uzrokuju fazni prijelaz jednako utječu na P_s i na spontani dvolom $\delta_s(\Delta n_c)$. P_s se ne mijenja za doze ispod kritične, $D < D_0$, ali za $D > D_0$ smanjuje se naglo. Ishodi mjerenja se raspravljaju na osnovi dvostrukog minimuma potencijala koji se rabi za opis feroelektričnog mehanizma. Koercitivno polje E_c i polarizacijsko polje E_b rastu s ozračivanjem zbog promjena unutarnjih polja. Električna vodljivost σ pokazuje anomaliju na kritičnoj temperaturi T_c zbog stvaranja protonskih nositelja koji su posljedica zakretanja kationa. Pri $D < D_0$, σ raste zbog povećanja broja pokretnih nositelja naboja velike pokretljivosti, ali se za $D > D_0$ smanjuje zbog djelovanja klopki.